

Supporting Information

Well-controlled Layer-by-Layer Assembly of Carbon Dots/ CdS Heterojunction for Efficient Visible-Light-Driven Photocatalysis

Na-Na Chai,^a Hang-Xing Wang,^a Chen-Xia Hu,^a Qiang Wang*^b and Hao-Li Zhang*^a

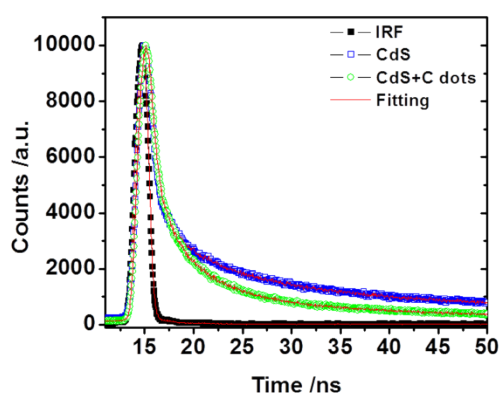


Figure S1 Time-resolved fluorescence spectra of bare CdS and CdS with addition of C dots solution.

Table S1. Fluorescence lifetimes of samples in aqueous solution. (Measured at $\lambda_{ex} = 360$ nm and $\lambda_{em} = 480$ nm)

Samples	χ^2	τ_1 (ns)	τ_2 (ns)	τ_3 (ns)	$\langle\tau\rangle$ (ns)	B1	B2	B3
CdS	1.14	0.7	7.7	44.5	4.0	0.059	0.008	0.004
CdS + C dots	1.15	0.9	5.7	37.4	3.0	0.049	0.012	0.002

$$\langle\tau\rangle = \frac{\sum_i B_i \tau_i}{\sum_i B_i} \quad \text{eqn(1)}$$

The averaged lifetimes were estimated using eqn (1), where τ_i and B_i are time constants and amplitudes, respectively. The magnitudes of lifetimes (τ_1 , τ_2 and τ_3) and the average lifetimes $\langle\tau\rangle$ are presented in Table S1.

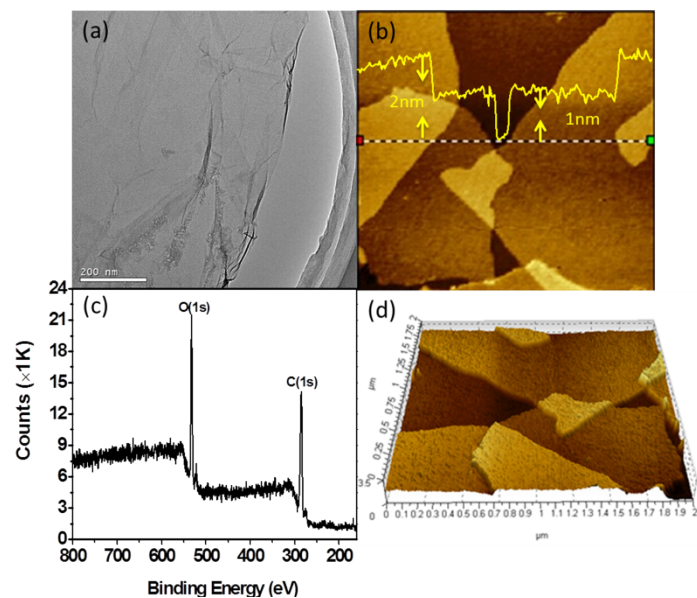


Figure S2 TEM images of (a) GO, AFM images of (b) GO, (c) XPS spectra of GO and (d) Cross section image of GO.

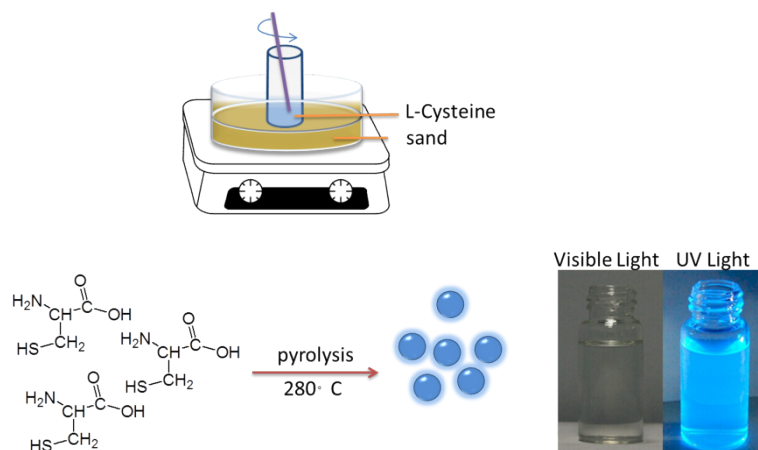


Figure S3. Schematic diagram of home-built reaction equipment and preparation of C dots.

Table S2 Energy band gaps of hybrid multilayers.

Samples	Eg (Band Gap)
(C Dots-CdS) ₃	2.43eV
(C Dots-CdS) ₅	2.25eV
(C Dots-CdS) ₆	2.14eV
(C Dots-CdS) ₇	2.05eV
CdS	2.33eV
(GO-CdS) ₆	1.30eV

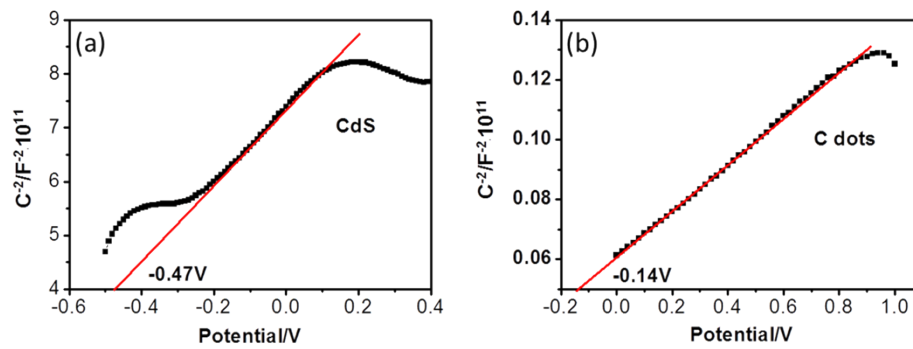


Figure S4. Mott-Schottky plots of (a) CdS and (b) C dots samples in 0.5 M Na₂SO₄ solution. (Potential vs. Ag/AgCl)

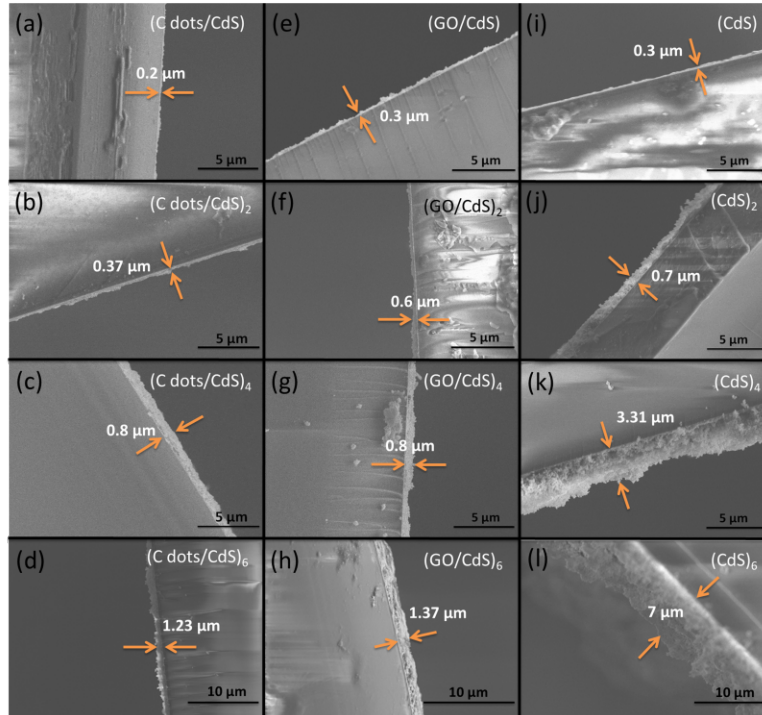


Figure S5 Cross-sectional SEM micrographs for 1, 2, 4 and 6 layers hybrid films.

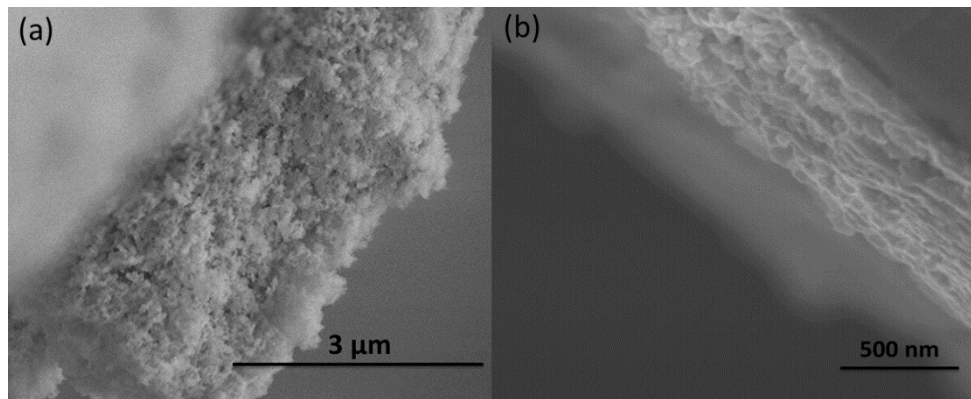


Figure S6 Cross-sectional SEM micrographs of (a) pure $(\text{CdS})_4$ and (b) $(\text{C dots/CdS})_4$.

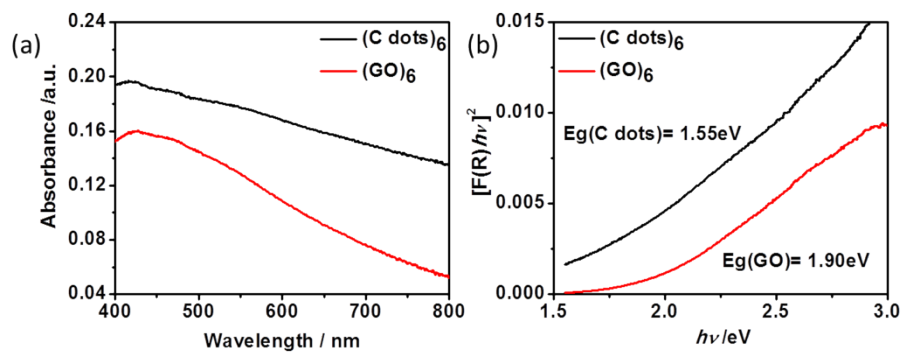


Figure S7. UV-vis absorption spectra of (a) $(\text{GO})_6$ and $(\text{C dots})_6$ films, and (b) plot of $[\text{F}(\text{R})h\nu]^2$ versus $h\nu$ for thin films.

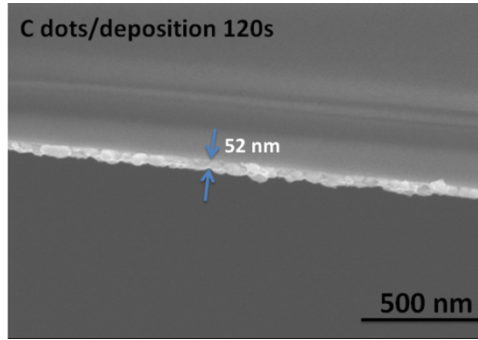


Figure S8. Cross-sectional SEM image for 120s deposition C dots layer.

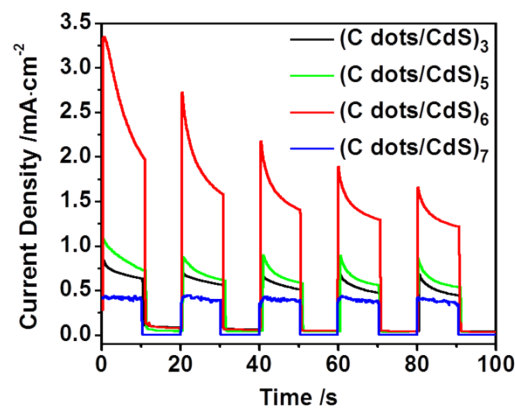


Figure S9. Transient photocurrent responses of these hybrid films in 0.05 M Na₂S aqueous solution at zero bias versus Pt counter electrode under 3W LED light irradiation (15.4mW/cm², $\lambda > 420\text{nm}$).

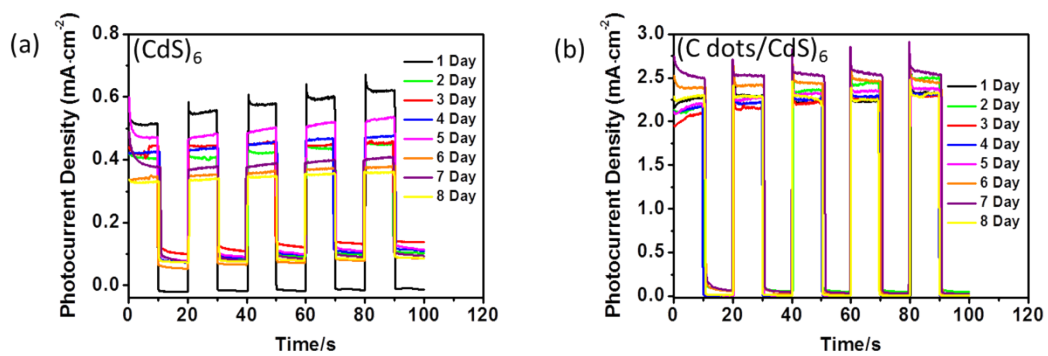


Figure S10. Transient photocurrent responses of these hybrid films from 1 to 8 days in 0.05 M Na₂S aqueous solution at zero bias versus Pt counter electrode under Xe light irradiation.

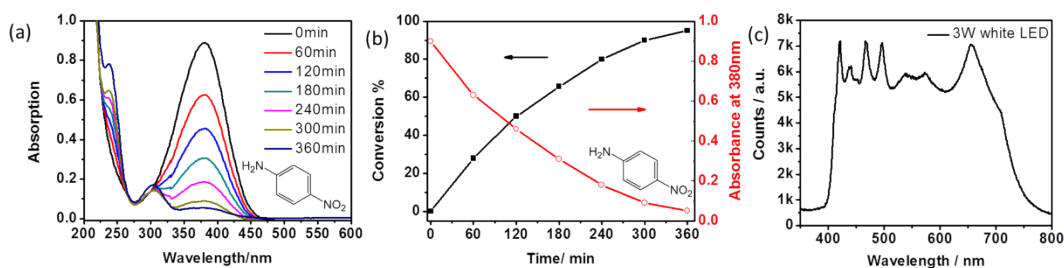


Figure S11. (a, b) Time-dependent UV-vis spectral variation during the photocatalytic reduction of P-nitroaniline over (C dots/CdS)₆. 20mg HCOONH₄ as quencher for photogenerated hole and N₂ purge at room temperature in the aqueous phase with 3W LED light (>420nm). (c) The optical range of LED (3W) light.

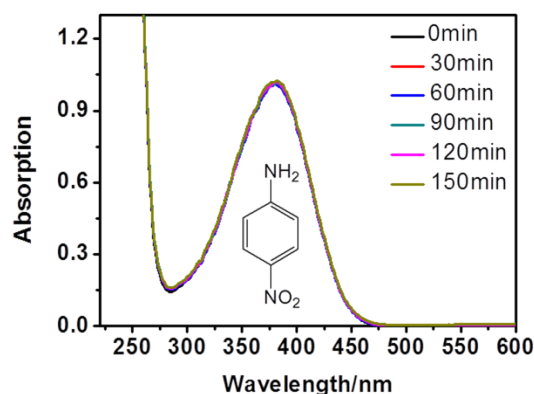


Figure S12. Time-dependent UV-vis spectral variation during the photocatalytic reduction of P-nitroaniline without photocatalyst (C dots/CdS)₆. 20mg HCOONH₄ as quencher for photogenerated hole and N₂ purge at room temperature in the aqueous phase with 3W LED light (>420nm).

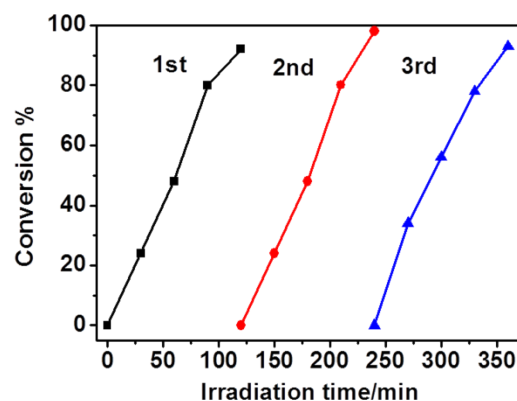


Figure S13. Cycling measurements of photocatalytic reduction of p-nitroaniline to p-phenylenediamine over (C dots/CdS)₆ composite film under the same experimental conditions.